Electronic Supplementary Material (ESI) for Dalton Transactions.

Supporting Information

A frontier-orbital view of the initial steps of the lytic polysaccharide monooxygenase reactions

Erna Katharina Wieduwilt,[a] Leila Lo Leggio[b] and Erik Donovan Hedegård*[a]

[a] *Department of Physics, Chemistry, and Pharmacy, University of Southern Denmark, Campusvej 55, 5230 Odense M, Denmark.*

[b] *Department of Chemistry, University of Copenhagen, 2100 Copenhagen, Denmark*

Contents

Table S1: Selected distances and angles for the structures shown in Figure 2, Figure S1, and Figure S8. Distances with only one atom are between the indicated atom and copper. For the equatorial and axial water ligands, the distance to oxygen is reported. In the case of two oxygen atoms in O_2 and H_2O_2, only the distance to the oxygen closer to copper is reported, while the distance between the two oxygen atoms is given in the last column. See Vu *et al.* for the definition of the angles θ_1, θ_2, θ_3 and θ_T.[1]

Structure	PDB entry	$N^{\delta 1}$ (Å)	N^{ter} (Å)	$N^{\varepsilon 2}$ (Å)	O_{Tyr} (Å)	Eq (Å)	Ax (Å)	θ_1, θ_2, θ_3 (°)	θ_T (°)	O-O (Å)
Cu(II)	7pxi	1.87	2.18	1.96	2.74	2.16	2.71	92.9, 89.6, 177.1	1.5	n/a
Cu(I)	7pxv	1.84	2.29	1.99	2.81	4.03	3.49	93.2, 97.4, 168.6	4.4	n/a
Cu(I)…H_2O_2	7pxv‡					2.54				1.50
Cu(I)…O_2	7pxv*					3.87				1.24
Cu(II)-O_2	7pxv*					2.27				1.27
Cu(II)-Cell-Cl^-	7pyd	2.00	2.26	2.02	2.48	2.25	n/a	96.4, 94.1, 161.1	15.6	n/a
Cu(II)-Cell	7pyd#									
Cu(II)-Cell-O_2	7pyd**					2.22				1.28
Cu(I)-Cell-Cl^-	7pyi	1.89	2.50	2.00	2.69	3.84	n/a	98.1, 110.1, 147.9	14.5	n/a
Cu(I)-Cell	7pyi#									
Cu(I)-Cell…H_2O_2	7pyi‡‡					2.39				1.72
Cu(I)-Cell…O_2	7pyi**					2.55				1.26

‡ The equatorial water (not in coordinating distance) is replaced with H_2O_2 and H_2O_2 is optimized

* The equatorial water (not in coordinating distance) is replaced with O_2 and O_2 is optimized (with Cu-O distance constraint in case of Cu(I)…O_2)

Chloride is replaced with H_2O and oxygen is constrained to the position of chloride

** Chloride is replaced with O_2, the 7pyd model is computationally reduced and O_2 is optimized

‡‡ Chloride is replaced with H_2O_2 and H_2O_2 is optimized

Table S2: Selected distances (in Å) for structures with O_2 and H_2O_2 (systems in green boxes in Figure 1). Structures are shown in Figure 2 and Figure S1.

O_2	$Cu-O^1_{O_2}$	$O^1_{O_2}-O^2_{O_2}$	$H^{\epsilon 2}_{His147}\dots O^2_{O_2}$	$H^{\epsilon 22}_{Gln162}\dots O^2_{O_2}$	
Cu(I)…O_2	3.87	1.24	2.20	2.18	
Cu(I)-Cell…O_2	2.55	1.26	1.92	2.60	
Cu(II)-O_2	2.27	1.27	2.60	2.54	
Cu(II)-Cell-O_2	2.22	1.28	2.04	2.07	
H_2O_2	$Cu-O^1_{H_2O_2}$	$O^1_{H_2O_2}-O^2_{H_2O_2}$	$H^{\epsilon 2}_{His147}\dots O^2_{H_2O_2}$	$H^{\epsilon 22}_{Gln162}\dots O^2_{H_2O_2}$	$O^{\epsilon 1}_{Gln162}\dots H^1_{H_2O_2}$
Cu(I)…H_2O_2 (Ref. [2])	2.93	1.46	2.00	1.97	1.75
Cu(I)…H_2O_2	2.54	1.50	1.92	1.83	1.87
Cu(I)-Cell…H_2O_2	2.39	1.72	2.07	1.82	1.93

Table S3: Löwdin spin populations for selected atoms and summed for all residues, obtained from B3LYP/def2-TZVPP calculations.

Atom/Residue	Cu(II)	Cu(II)-Cell	Cu(II)-Cell-Cl^-	Cu(I)…O_2	Cu(I)-Cell…O_2	Cu(II)-O_2	Cu(II)-Cell-O_2
N^{ter}	0.12	0.13	0.07	0.01	0.02	0.04	0.05
$N^{\delta 1}$	0.06	0.05	0.06	0.01	0.02	0.03	0.04
Sum His1	0.23	0.25	0.16	0.03	0.06	0.10	0.12
$N^{\varepsilon 2}$	0.06	0.05	0.08	0.00	0.02	0.03	0.04
Sum His78	0.06	0.06	0.09	0.00	0.02	0.04	0.05
Sum His147	0.00	0.00	0.00	0.01	0.02	0.00	0.02
Sum Gln162	0.00	0.00	0.00	0.01	0.01	0.00	0.00
Sum Tyr164	0.00	0.02	0.00	0.00	0.00	0.00	0.00
Cu	0.65	0.62	0.60	0.07	0.22	0.37	0.45
O1/Cl	0.05	0.04	0.15	0.97	0.90	0.76	0.72
O2	n/a	n/a	n/a	0.91	0.76	0.73	0.65
Sum eq. ligand	0.05	0.04	0.15	1.89	1.66	1.49	1.37
Sum ax. ligand	0.00	n/a	n/a	0.00	n/a	0.00	n/a
Sum pkt. water	0.00	0.00	0.00	0.00	0.00	0.00	0.00
Sum substrate	n/a	0.00	0.00	n/a	0.01	n/a	0.00

Table S4: QTAIM atomic charges for copper and summed for all residues, obtained from B3LYP/def2-TZVPP calculations.

Atom/Residue	Cu(II)	Cu(I)	Cu(II)-Cell	Cu(I)-Cell	Cu(I)…H_2O_2	Cu(I)-Cell…H_2O_2
Sum His1	0.45	0.22	0.47	0.20	0.22	0.24
Sum His78	0.22	0.16	0.22	0.13	0.17	0.18
Sum His147	0.01	-0.01	0.01	-0.01	-0.01	0.00
Sum Gln162	0.08	0.03	0.07	0.02	0.04	0.04
Sum Tyr164	0.02	-0.01	0.03	0.00	-0.01	0.00
Cu	1.15	0.61	1.10	0.64	0.68	0.77
Sum eq. ligand	0.01	-0.02	0.02	-0.01	-0.09	-0.25
Sum ax. ligand	0.04	0.00	n/a	n/a	n/a	n/a
Sum pkt. water	0.02	0.00	0.02	-0.01	-0.01	-0.01
Sum substrate	n/a	n/a	0.08	0.03	n/a	0.02

S1. Impact of pre-bound oxygen vs. superoxide

Investigated Structures with O_2. For comparison with previous studies,[3, 4] we investigated if the substrate could induce changes to the electronic structure of a dioxygen-bound intermediate. Previous computational studies[3, 5, 6] demonstrated that it is more favourable for oxygen to bind in the equatorial than in the axial position and that a triplet state is more stable than the open-shell singlet for all $[CuO_2]^+$ intermediates, irrespective of substrate binding. Therefore, we calculated Cu(II)-O_2 (without substrate) and Cu(II)-Cell-O_2 (with substrate) intermediates with O_2 in the equatorial position and in a triplet state. This intermediate is usually described as a $O_2^{\bullet-}$ superoxide bound to Cu(II).[3, 5-9] For comparison with the pre-bound H_2O_2 structures presented in the main paper, we further calculated two pre-bound states: Cu(I)…O_2 (without substrate) and Cu(I)-Cell…O_2 (with substrate). All four investigated structures with O_2 are shown in Figure S1.

Computational Details. From the Cu(I) structure, the structure labelled Cu(II)-O_2 was obtained. The coordinates of O_2 were freely optimized together with the hydrogen atoms using the procedure described in the Computational Details in the main text. To obtain the pre-bound Cu(I)…O_2, the Cu-O distance (of 2.27 Å) in Cu(II)-O_2 was elongated in steps of 0.2 Å and a local minimum was found at 4.8 Å (see Figure S2). Note that O_2 is turned in comparison to the pre-bound Cu(I)…O_2 and that the Cu-O distance to the closer oxygen is 3.87 Å at the local minimum structure. When the Cu-O distance is unconstraint, the superoxide state is retained.
For the structures with a substrate, the Cu(II)-Cell-Cl^- structure (with chloride bound) has been postulated to be a mimic[10] for the $[CuO_2]^+$ intermediate. Considering that this intermediate is often described as a $O_2^{\bullet-}$ superoxide bound to Cu(II).[3, 5-9], there are two ways to generate the $[CuO_2]^+$ species when the substrate is bound: (i) we can add O_2 to the Cu(I)-Cell-Cl^- structure, replacing Cl^- with O_2 or (ii) we can add $O_2^{\bullet-}$ to the Cu(II)-Cell-Cl^- structure (again replacing Cl^-). We investigated both possibilities (i) and (ii). In both cases, we freely optimized the positions of O_2 /$O_2^{\bullet-}$ and all hydrogen atoms, while constraining the remaining atoms at the crystal structure positions. The structure obtained following way (ii) is 76.6 kJ/mol lower in energy than the one resulting from way (i) (based on B3LYP/def2-TZVPP calculations). Thus, the Cu(II)-Cell-Cl^- structure is presumably a good structural model for the superoxide species. The structure obtained following way (ii) will be labelled Cu(II)-Cell-O_2, as the Cu-O distance is 2.22 Å, which is somewhat longer than the distances of approximately 2 Å obtained from previous calculations.[5-7, 9] On the other hand, the Cu-O distance is with 2.55 Å even longer in the structure obtained following way (i). This structure will be labelled Cu(I)-Cell…O_2 and represents the pre-bound O_2 structure with substrate.

Electronic Structure of Pre-Bound Cu(I)…O_2 and Cu(I)-Cell…O_2. The orbital splitting diagrams for Cu(I)…O_2, and Cu(I)-Cell…O_2 are shown in Figure S3 for B3LYP (and Figure S11 for TPSS). Despite their open-shell structure, we observe similarities to the pre-bound Cu(I)…H_2O_2 and Cu(I)-Cell…H_2O_2: the occupied orbitals of copper d-character are in both structures close to the frontier. In Cu(I)…O_2, the α-HOMO is a ligand orbital located on tyrosine, but the α-HOMO-1 and the β-HOMO are orbitals of copper d-character (see Table S13). More precisely, the latter are the d_{x2-y2}-orbitals shown in Figure S5. The next

lower-lying MOs of copper d-character are 1.2-1.9 eV lower in energy than the d_{x2-y2}-orbitals, which is comparable to the 1.2-1.7 eV energy difference obtained for Cu(I)…H_2O_2 (see Table S13 and S11, respectively).

Substrate binding has similar effects on the occupied orbitals in both pre-bound Cu(I)-Cell…H_2O_2 and Cu(I)-Cell…O_2: the HOMO is in all cases ligand-based (see Table S11 and S13), and the d_{x2-y2}-orbitals are the highest lying copper d-orbitals (see Figure S3 and S5). The energy difference from the d_{x2-y2}-orbitals to the next lower-lying copper d-MOs is 0.5-1.8 eV in Cu(I)-Cell…O_2. Thus, we observe that substrate binding brings the d_{x2-y2}-orbitals and the lower-lying Cu d-orbitals closer together, which is consistent with our observations for the Cu(I) and pre-bound H_2O_2 systems and the observations by Lim *et al*[2].

In both Cu(I)…O_2 and Cu(I)-Cell…O_2, the β-LUMO and β-LUMO+1 orbitals (see Figure S5) are O_2 π*-orbitals. Interestingly and in contrast to Cu(I)…H_2O_2, we observe that the β-LUMO and β-LUMO+1 are raised in energy upon substrate binding in Cu(I)-Cell…O_2.

Comparison Between Pre-Bound O_2 and Bound Superoxide. Contrary to the observed changes upon substrate binding for pre-bound O_2 and H_2O_2, we find that substrate binding has only a minor impact on the electronic structure when the superoxide is bound: The frontier MOs in Cu(II)-O_2 and Cu(II)-Cell-O_2 have the same character and splittings in the presence and absence of substrate (see Figures S4 and S12). They are a mixture of ligand-based orbitals, oxygen or mixed oxygen/copper orbitals (see Tables S15 and S16). Compared to the pre-bound Cu(I)…O_2 and Cu(I)-Cell…O_2, the occupied copper d-orbitals are shifted further away from the frontier in Cu(II)-O_2 and Cu(II)-Cell-O_2, albeit not as much as before the reduction (compare to Figure 3 and S10). The HOMO-LUMO gap is the smallest in the structure with the longest Cu-O distance (namely Cu(I)…O_2) and increases when the closer oxygen approaches copper. We observe that the spin density is in all four structures mainly located on O_2, and the shorter the Cu-O distance, the more spin density is redistributed from O_2 to copper (see Table S3 and Figure S7).

Conclusions. Based on our observations for both the pre-bound O_2 and the superoxide, we currently cannot confirm the suggestion[4] by Courtade *et al.* that the substrate causes the d_{x2-y2}-orbital to be energetically closer to the anti-bonding O_2 π*-orbital. Instead, we observe that the energy difference between these orbitals increases as O_2 binds to copper. However, we do observe that the substrate causes the d_{x2-y2}-orbital to be energetically closer to the anti-bonding H_2O_2 σ*-orbital, when H_2O_2 instead of O_2 is pre-bound to the LPMO.

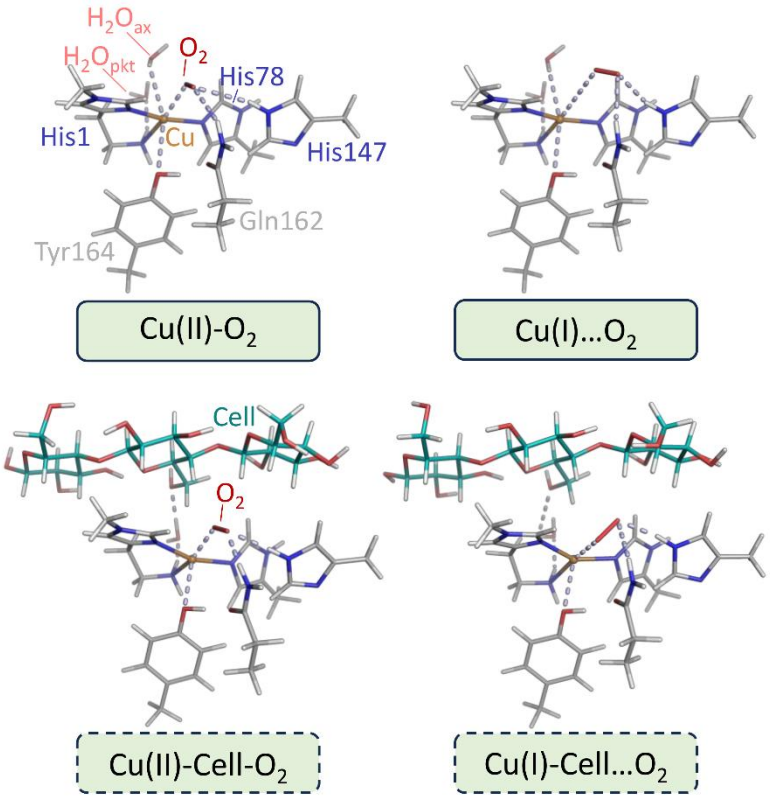

Figure S1: Structures with bound and pre-bound O_2 (corresponding to reactants and products of reactions 4a and 4b in Figure 1).

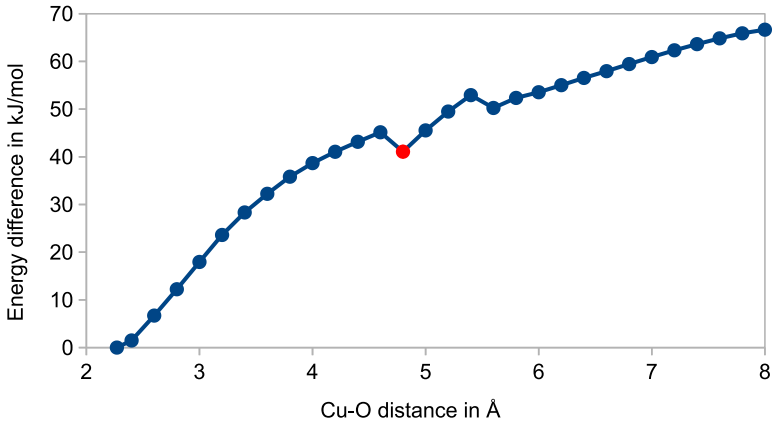

Figure S2: Energy difference associated with increasing the distance between O_2 and Cu. The structure corresponding to the local minimum marked in red was taken as the pre-bound Cu(I)…O_2 structure.

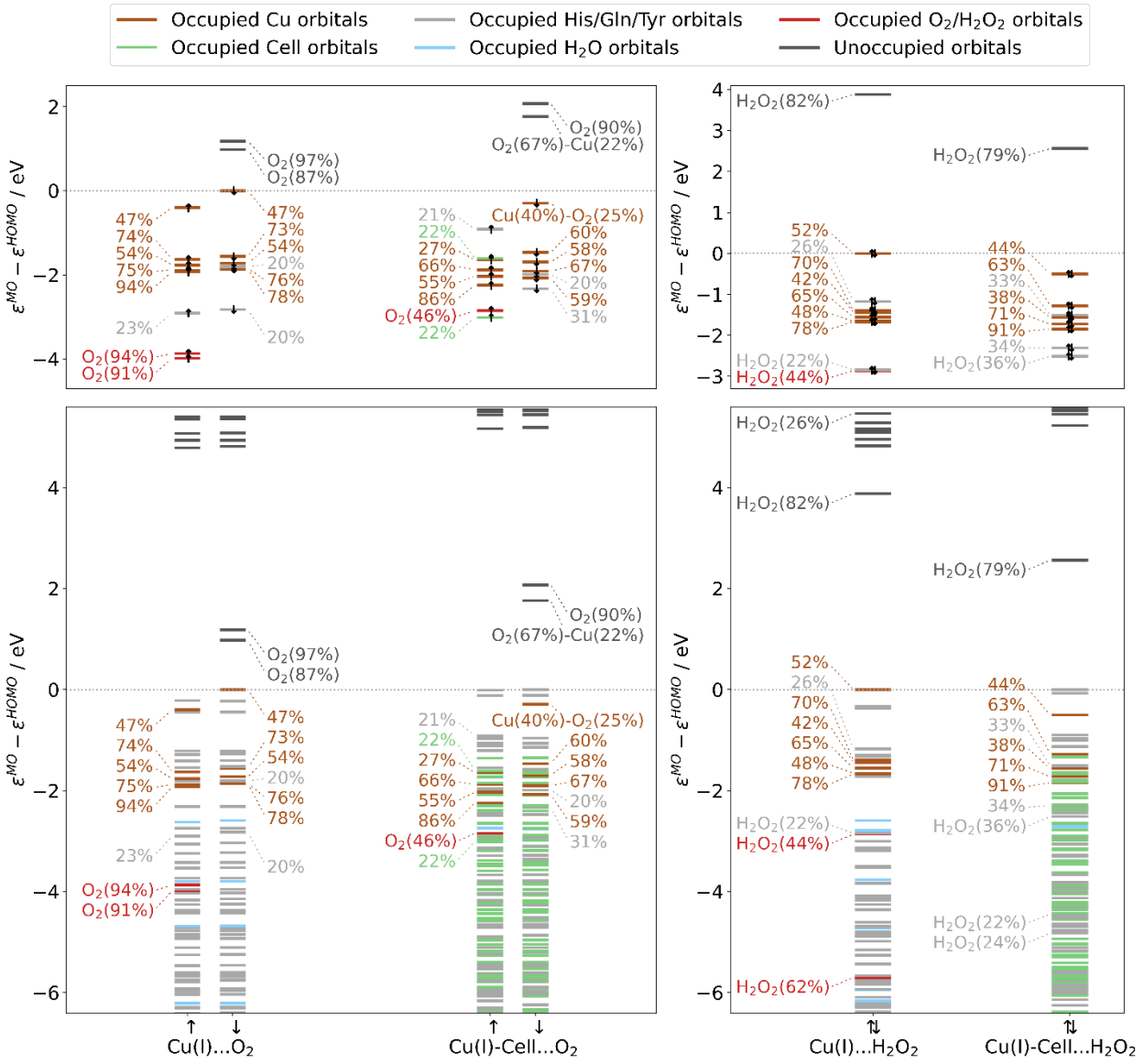

Figure S3: Normalized orbital energies and Löwdin reduced orbital populations per molecular orbital for substrate-free and substrate-bound structures with pre-bound O_2 (left panels) and H_2O_2 (right panels), obtained from B3LYP/def2-TZVPP calculations (and obtained from adding O_2 or H_2O_2 to the crystal structures, see green boxes in Figure 1). The colour indicates the residue with the largest Löwdin reduced orbital population (see legend). Löwdin reduced orbital population are reported if the population of the copper d-orbitals (here only numbers are given), O_2 and H_2O_2 orbitals is larger than 20%. Only these orbitals are shown in the top panels, whereas the bottom panels include all orbitals. The orbital energies are normalized to the HOMO energy.

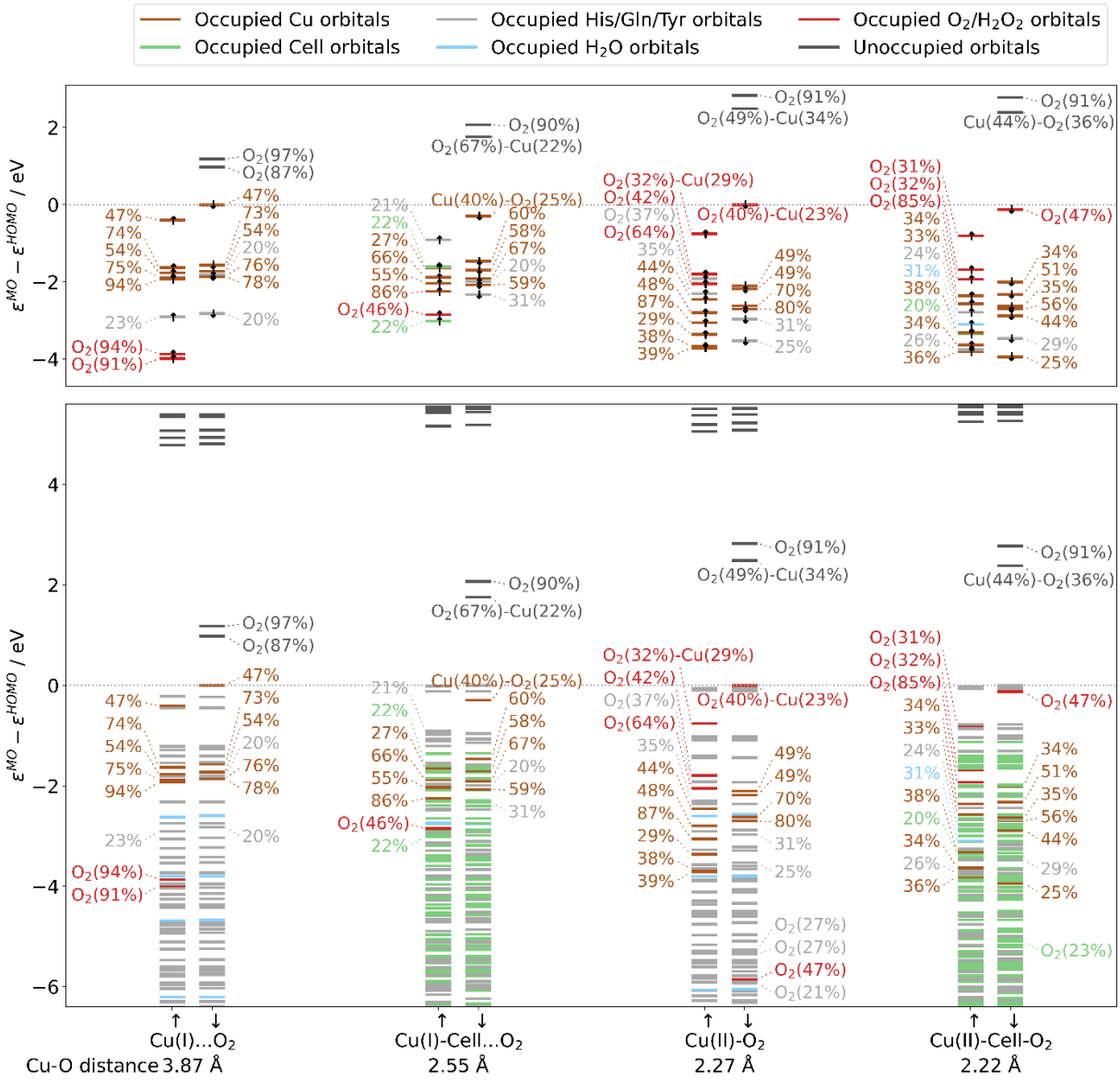

Figure S4: Normalized orbital energies and Löwdin reduced orbital populations per molecular orbital for substrate-free and substrate-bound structures with pre-bound O_2 (left) and bound O_2 (right), obtained from B3LYP/def2-TZVPP calculations (and obtained from adding O_2 to the crystal structures, see green boxes in Figure 1). The colour indicates the residue with the largest Löwdin reduced orbital population (see legend). Löwdin reduced orbital population are reported if the population of the copper d-orbitals (here only numbers are given), and O_2 orbitals is larger than 20%. Only these orbitals are shown in the top panel, whereas the bottom panel includes all orbitals. The orbital energies are normalized to the HOMO energy.

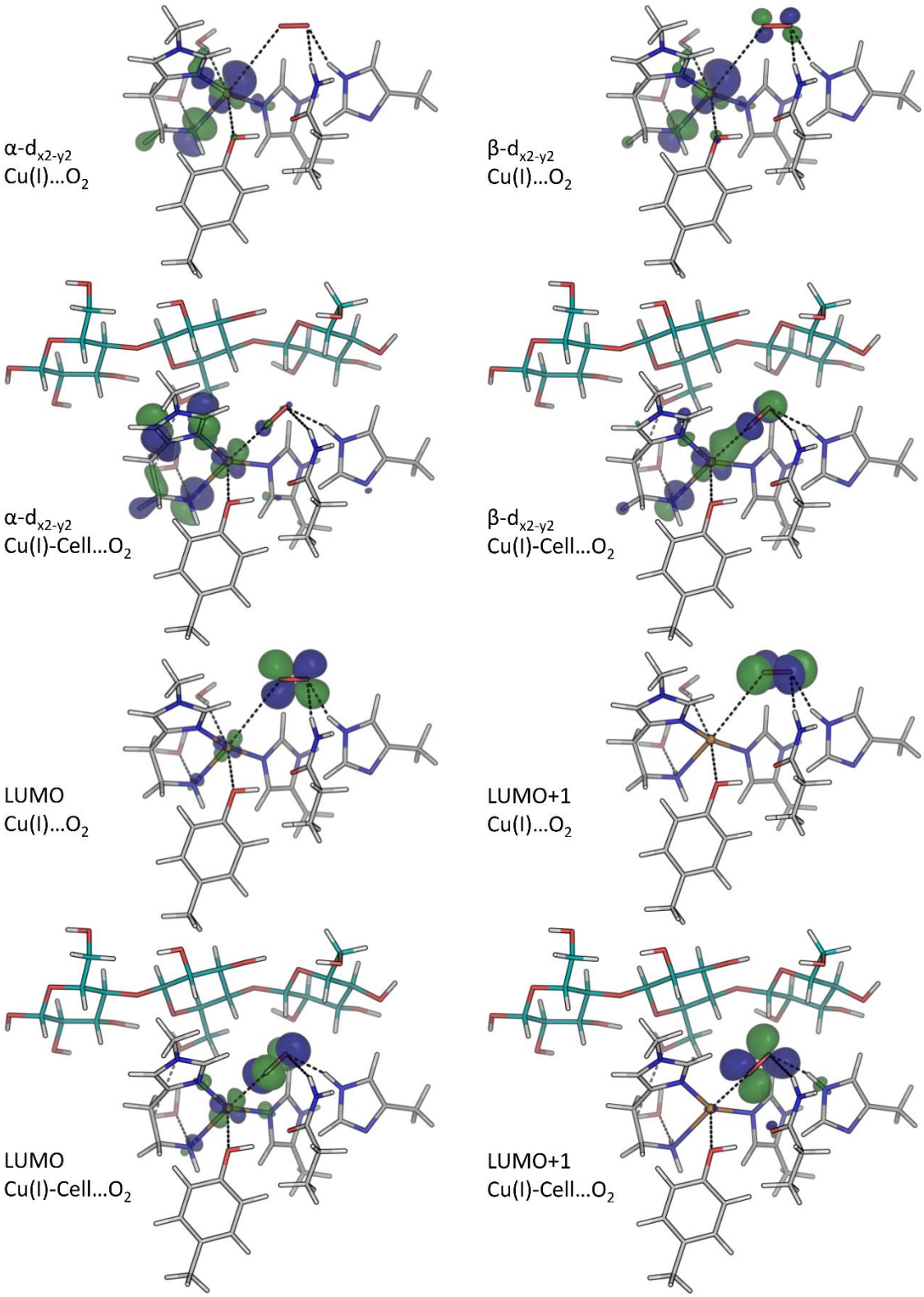

Figure S5: Selected orbitals (isovalue 0.05 e/bohr^3) for structures with pre-bound O_2, obtained from B3LYP/def2-TZVPP calculations.

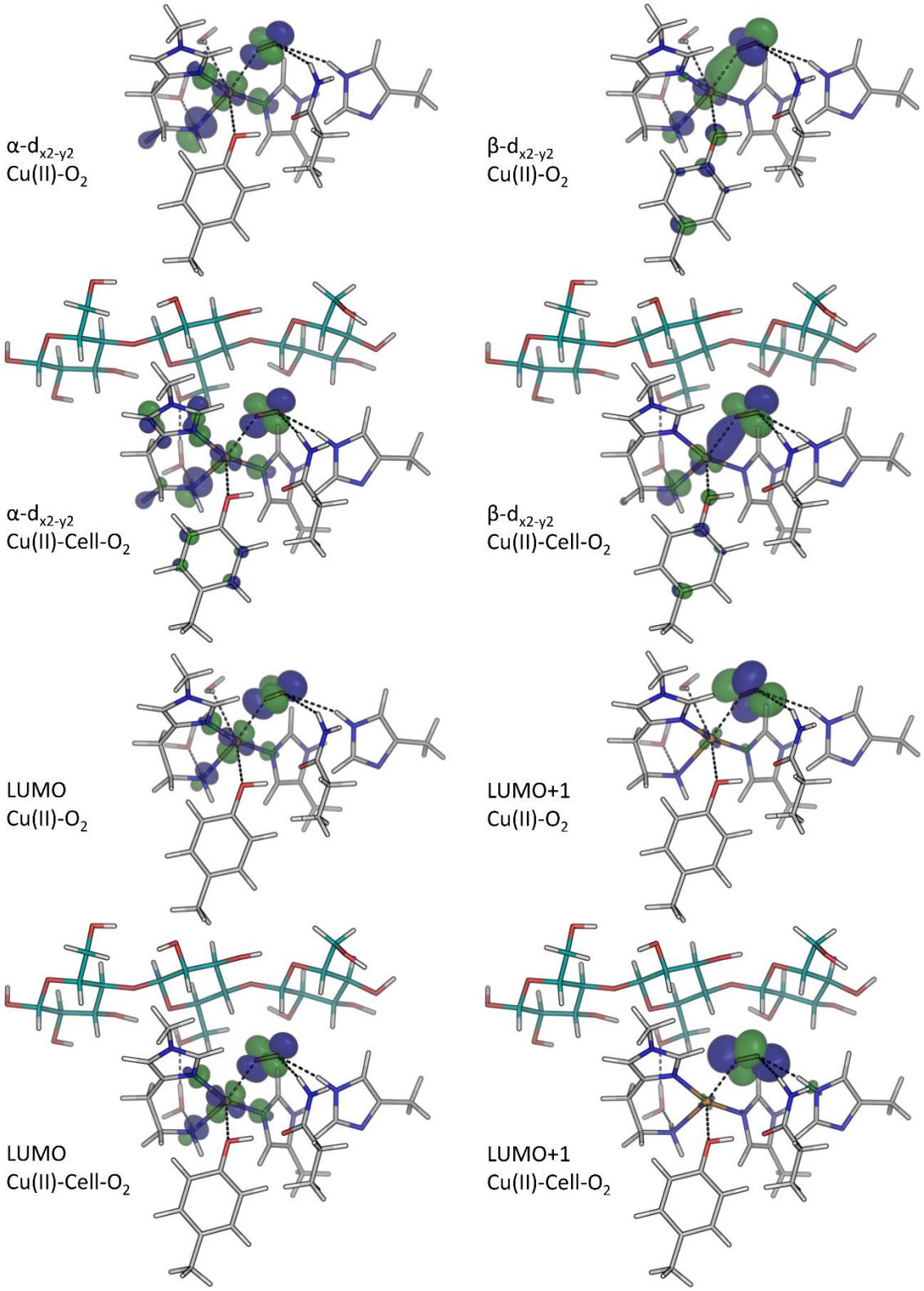

Figure S6: Selected orbitals (isovalue 0.05 e/bohr^3) for structures with bound O_2, obtained from B3LYP/def2-TZVPP calculations.

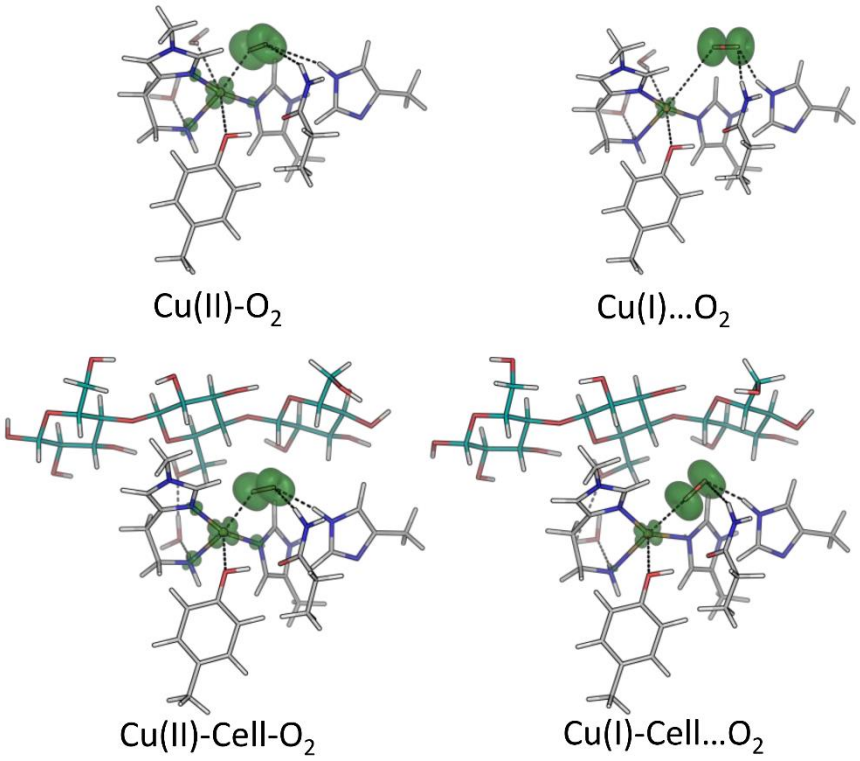

Figure S7: Spin densities for structures with bound and pre-bound O_2, obtained from B3LP/def2-TZVPP calculations (isovalue 0.01 e/bohr^3). The spin density is defined as the difference in the densities contributed by the α and β-electrons.

S2. Impact of chloride

All crystal structures with substrate contain a chloride anion (see Figure S8). In the main text, we chose to investigate systems where the chloride ions observed in all substrate-bound X-ray structures were replaced with water. The main reason is that the presence of the chloride has a non-negligible impact on the electronic structure, as additional superhyperfine couplings appear in the EPR spectra if these are measured after the addition of substrate and under high-chloride conditions.[10] As shown in Figure S9, chloride carries spin density in the Cu(II)-Cell-Cl^- structure (the Löwdin spin population is 0.15, see Table S3). In the same structure, the occupied chloride orbitals are not the frontier orbitals (see Figure S9), but they are either energetically closer to the frontier than the occupied copper d-orbitals (for the B3LYP calculation) or most occupied copper d-orbitals (for the TPSS calculation). In Cu(I)-Cell-Cl^-, the reduction brings the occupied copper orbitals closer to the frontier than the occupied chloride orbitals, showing again the large impact of the reduction on the electronic structure.

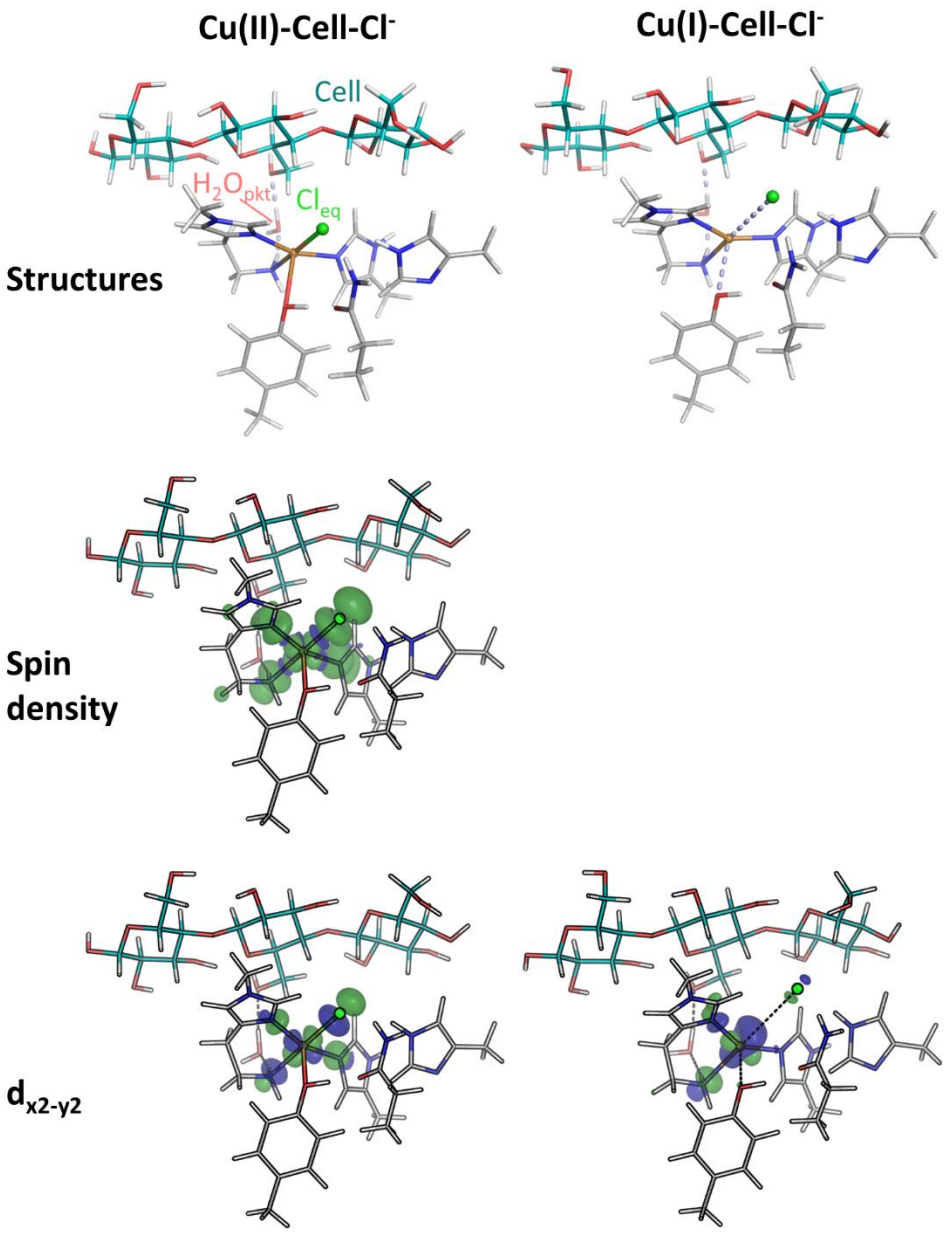

Figure S8: Model structures including chloride (top). Spin density (middle, isovalue 0.001 e/bohr^3) and d_{x2-y2} orbitals (bottom, isovalue 0.05 e/bohr^3) obtained from B3LYP/def2-TZVPP calculations. In both cases, green colour corresponds to positive values, and blue to negative ones. The spin density is defined as the difference in the densities contributed by the α and β-electrons. The d_{x2-y2} orbital in Cu(II)-Cell-Cl$^-$ is the LUMO and the highest occupied d-orbital in Cu(I)-Cell-Cl$^-$.

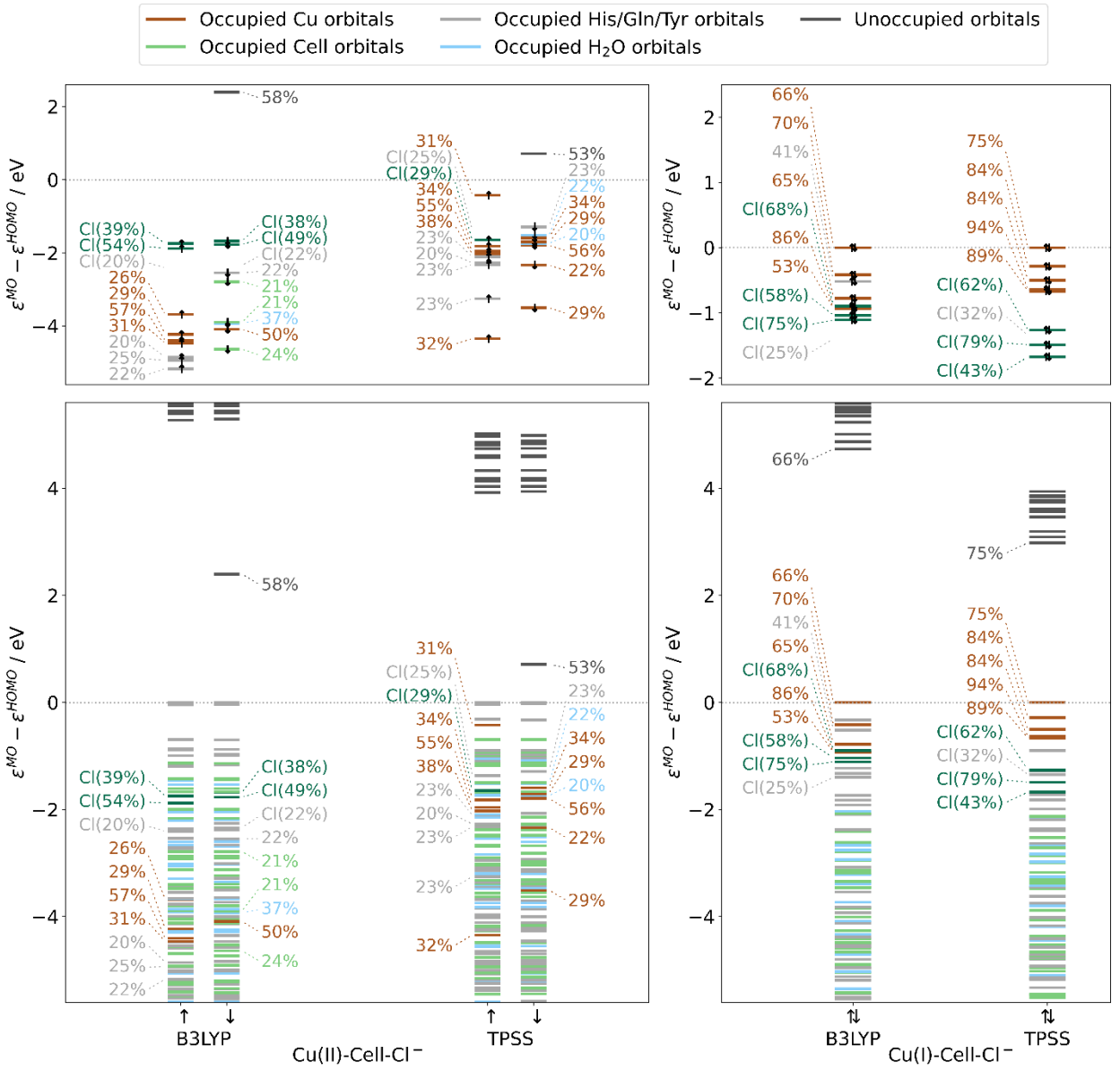

Figure S9: Normalized orbital energies and Löwdin reduced orbital populations per molecular orbital for Cu(II)-Cell-Cl$^-$ and Cu(I)-Cell-Cl$^-$ structures with chloride obtained from B3LYP/def2-TZVPP and TPSS/def2-TZVPP calculations as indicated. The colour indicates the residue with the largest Löwdin reduced orbital population (see legend). Löwdin reduced orbital population are reported if the population of the copper d-orbitals (here only numbers are given) and chloride orbitals is larger than 20%. Only these orbitals are shown in the top panels, whereas the bottom panels include all orbitals. The orbital energies are normalized to the HOMO energy.

S3. Results with TPSS

Table S5: Löwdin spin populations for selected atoms and summed for all residues, obtained from TPSS/def2-TZVPP calculations.

Atom/Residue	Cu(II)	Cu(II)-Cell	Cu(II)-Cell-Cl^-	Cu(I)…O_2	Cu(I)-Cell…O_2	Cu(II)-O_2	Cu(II)-Cell-O_2
N^{ter}	0.14	0.11	0.08	0.03	0.03	0.05	0.05
$N^{\delta 1}$	0.06	0.05	0.06	0.01	0.02	0.03	0.04
Sum His1	0.26	0.22	0.19	0.06	0.08	0.10	0.12
$N^{\varepsilon 2}$	0.06	0.05	0.09	0.01	0.02	0.03	0.04
Sum His78	0.07	0.06	0.10	0.01	0.02	0.04	0.06
Sum His147	0.00	0.00	0.00	0.01	0.03	0.00	0.02
Sum Gln162	0.00	0.00	0.00	0.01	0.02	0.00	0.00
Sum Tyr164	0.04	0.14	0.00	0.00	0.00	0.00	0.00
Cu	0.57	0.48	0.53	0.15	0.25	0.34	0.39
O1/Cl	0.05	0.03	0.17	0.91	0.86	0.76	0.73
O2	n/a	n/a	n/a	0.86	0.74	0.75	0.67
Sum eq. ligand	0.06	0.04	0.17	1.77	1.60	1.50	1.41
Sum ax. ligand	0.00	n/a	n/a	0.00	n/a	0.00	n/a
Sum pkt. water	0.00	0.00	0.00	0.00	0.00	0.00	0.00
Sum substrate	n/a	0.06	0.00	n/a	0.01	n/a	0.01

Table S6: QTAIM atomic charges for copper and summed for all residues, obtained from TPSS/def2-TZVPP calculations.

Atom/Residue	Cu(II)	Cu(I)	Cu(II)-Cell	Cu(I)-Cell	Cu(I)…H_2O_2	Cu(I)-Cell…H_2O_2
Sum His1	0.48	0.23	0.43	0.19	0.23	0.26
Sum His78	0.22	0.16	0.21	0.13	0.17	0.18
Sum His147	0.01	-0.01	0.01	0.00	-0.01	0.00
Sum Gln162	0.09	0.04	0.07	0.03	0.05	0.04
Sum Tyr164	0.05	-0.01	0.14	-0.01	0.00	0.00
Cu	1.07	0.61	0.98	0.64	0.70	0.81
Sum eq. ligand	0.02	-0.02	0.01	-0.01	-0.14	-0.32
Sum ax. ligand	0.04	0.00	n/a	n/a	n/a	n/a
Sum pkt. water	0.02	0.00	0.02	-0.01	-0.01	-0.01
Sum substrate	n/a	n/a	0.13	0.03	n/a	0.04

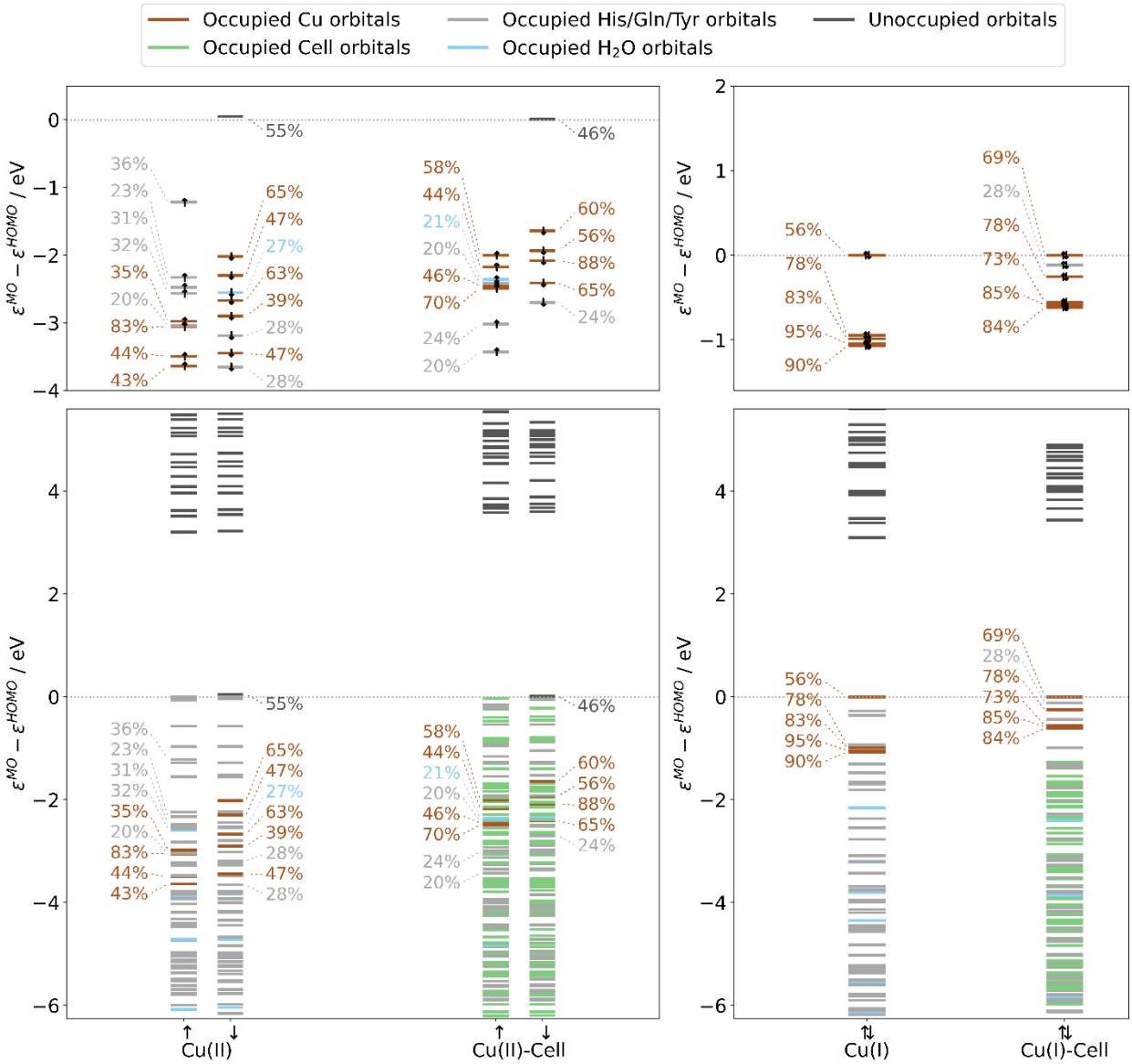

Figure S10: Normalized orbital energies and Löwdin reduced orbital populations per molecular orbital for Cu(II) and Cu(II)-Cell (left panels) as well as Cu(I) and Cu(I)-Cell structures (right panels), obtained from TPSS/def2-TZVPP calculations (and directly derived from the crystal structures, see blue boxes in Figure 1). The colour indicates the residue with the largest Löwdin reduced orbital population (see legend). Löwdin reduced orbital populations are reported if the population of the copper d-orbitals is larger than 20%. Only these orbitals are shown in the top panels, whereas the bottom panels include all orbitals. The orbital energies are normalized to the HOMO energy.

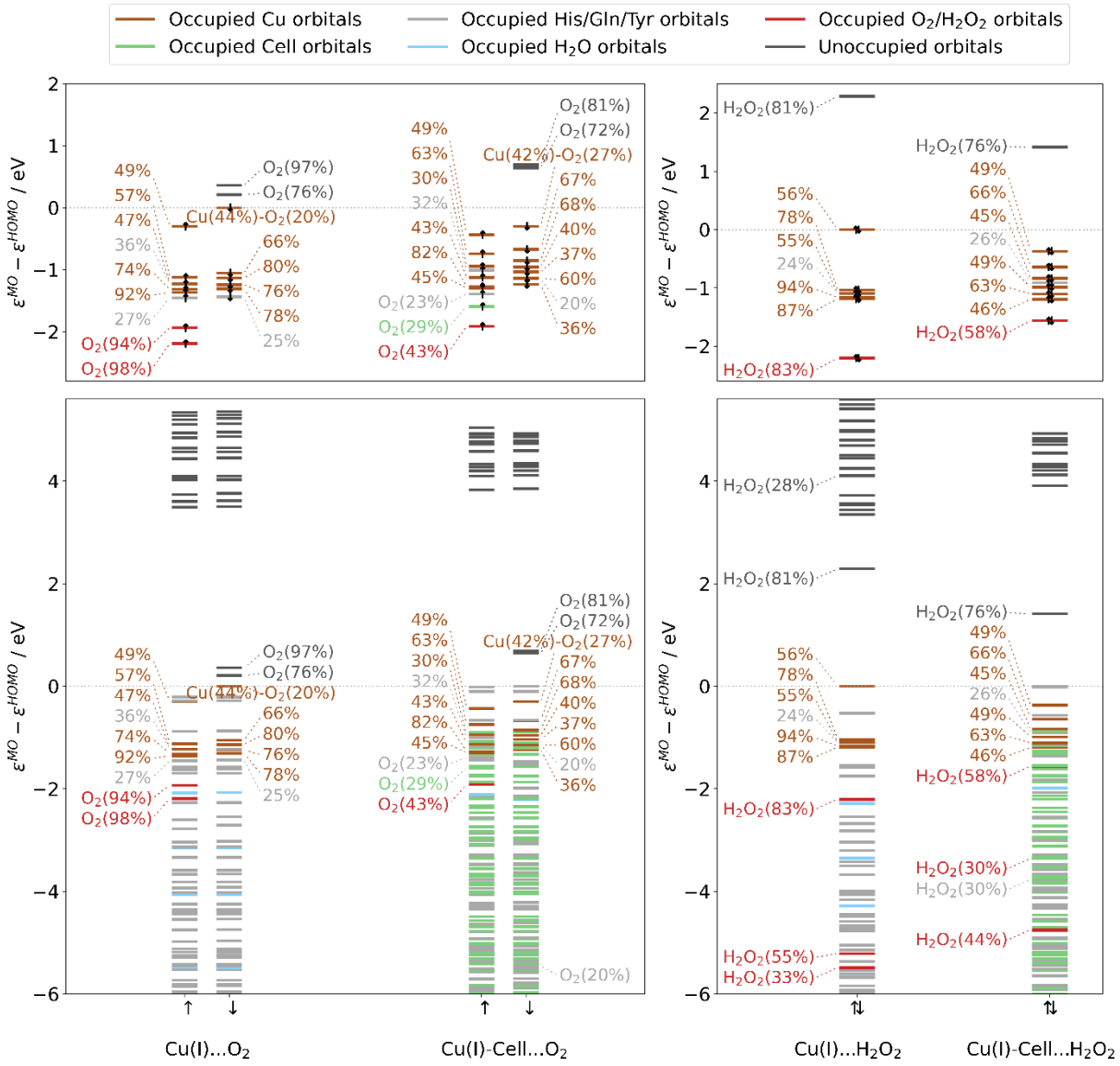

Figure S11: Normalized orbital energies and Löwdin reduced orbital populations per molecular orbital for substrate-free and substrate-bound structures with O_2 (left panels) and H_2O_2 (right panels), obtained from TPSS/def2-TZVPP calculations (and obtained from adding O_2 or H_2O_2 to the crystal structures, see green boxes in Figure 1). The colour indicates the residue with the largest Löwdin reduced orbital population (see legend). Löwdin reduced orbital population are reported if the population of the copper d-orbitals (here only numbers are given), O_2 and H_2O_2 orbitals is larger than 20%. Only these orbitals are shown in the top panels, whereas the bottom panels include all orbitals. The orbital energies are normalized to the HOMO energy.

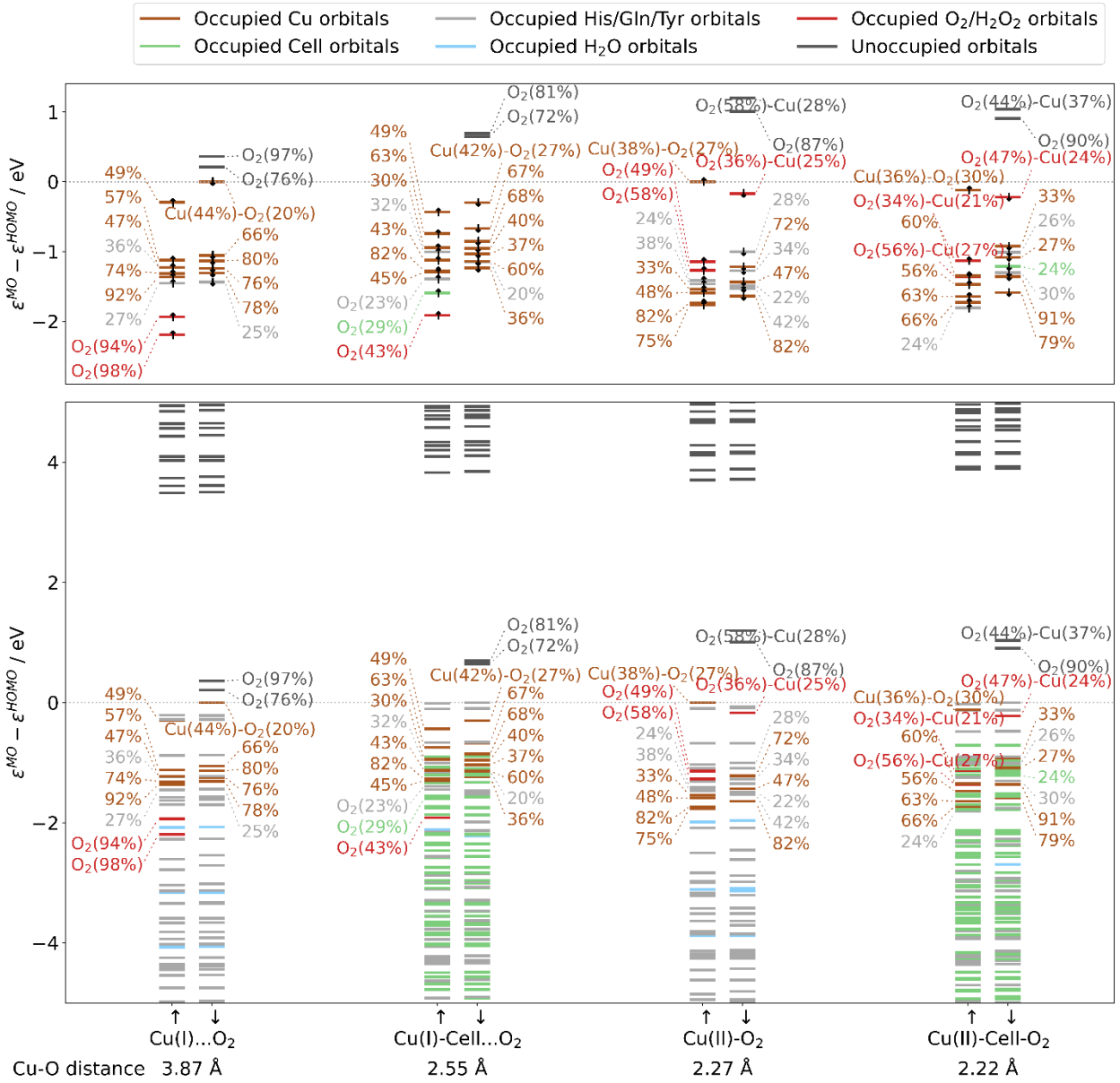

Figure S12: Normalized orbital energies and Löwdin reduced orbital populations per molecular orbital for substrate-free and substrate-bound structures with pre-bound O_2 (left) and bound O_2 (right), obtained from TPSS/def2-TZVPP calculations (and obtained from adding O_2 to the crystal structures, see green boxes in Figure 1). The colour indicates the residue with the largest Löwdin reduced orbital population (see legend). Löwdin reduced orbital population are reported if the population of the copper d-orbitals (here only numbers are given), and O_2 orbitals is larger than 20%. Only these orbitals are shown in the top panel, whereas the bottom panel includes all orbitals. The orbital energies are normalized to the HOMO energy.

S4. Selected orbital energies and Löwdin Reduced Orbital Populations

Table S7: Copper orbitals with significant d-orbital contribution, HOMO and LUMO in Cu(II) calculated with B3LYP/def2-TZVPP.

Orbital #	Frontier Orbital #	Occupation	ε^{MO}-ε^{HOMO} / eV	Löwdin Reduced Orbital Population	Cu-d Löwdin Reduced Orbital Population / %
			alpha		
92	HOMO-63	1	-8.2	His1(38%) His78(24%) Cu(21%) Gln162(10%)	20
116	HOMO-39	1	-5.6	His1(34%) His78(26%) Cu(22%) Wat(12%)	22
119	HOMO-36	1	-5.5	Cu(35%) His78(28%) His1(15%) Wat(11%)	34
122	HOMO-33	1	-5.3	Wat(43%) Cu(22%) His1(12%) His78(12%)	22
123	HOMO-32	1	-5.2	Cu(57%) His1(20%)	56
124	HOMO-31	1	-5.1	Cu(59%) His1(16%)	59
126	HOMO-29	1	-4.9	Cu(29%) His1(27%) Wat(21%) Tyr(17%)	28
131	HOMO-24	1	-4.4	Wat(33%) Cu(26%) His1(16%) Tyr(12%)	25
136	HOMO-19	1	-4.0	Cu(29%) His1(28%) Tyr(13%) His78(12%) Wat(10%)	25
148	HOMO-7	1	-2.2	His1(54%) Cu(24%)	23
155	HOMO	1	0.0	Tyr(96%)	0
156	LUMO	0	4.4	His78(49%) Wat(26%)	1

Table S7 (continued): Copper orbitals with significant d-orbital contribution, HOMO and LUMO in Cu(II) calculated with B3LYP/def2-TZVPP.

Orbital #	Frontier Orbital #	Occupation	ε^{MO}-ε^{HOMO} / eV	Löwdin Reduced Orbital Population	Cu-d Löwdin Reduced Orbital Population / %
			beta		
122	HOMO-32	1	-5.2	His78(34%) His1(26%) Cu(22%) Wat(12%)	21
123	HOMO-31	1	-4.9	Cu(37%) His1(25%) Wat(20%)	36
124	HOMO-30	1	-4.8	Cu(37%) Tyr(23%) His1(19%) Wat(11%)	37
125	HOMO-29	1	-4.8	Cu(39%) His1(38%) His78(11%)	39
130	HOMO-24	1	-4.5	Cu(74%) Wat(14%)	74
135	HOMO-19	1	-4.0	Cu(56%) His1(14%) Wat(14%)	55
154	HOMO	1	0.0	Tyr(96%)	0
155	LUMO	0	1.7	Cu(64%) His1(20%)	62

Table S8: Copper orbitals with significant d-orbital contribution, HOMO and LUMO in Cu(I) calculated with B3LYP/def2-TZVPP.

Orbital #	Frontier Orbital #	Occupation	ε^{MO}-ε^{HOMO} / eV	Löwdin Reduced Orbital Population	Cu-d Löwdin Reduced Orbital Population / %
144	HOMO-11	2	-1.7	Cu(90%)	90
145	HOMO-10	2	-1.6	Cu(64%) His78(20%) His1(12%)	64
146	HOMO-9	2	-1.5	Cu(62%) His1(28%)	62
148	HOMO-7	2	-1.4	Cu(75%) His1(17%)	73
149	HOMO-6	2	-1.4	His1(45%) Cu(31%) His147(12%)	29
154	HOMO-1	2	-0.1	Cu(48%) His1(26%) Tyr(15%)	40
155	HOMO	2	0.0	Tyr(77%) Cu(13%)	11
156	LUMO	0	4.4	Wat(51%) Cu(20%) His78(11%)	10

Table S9: Copper orbitals with significant d-orbital contribution, HOMO and LUMO in Cu(II)-Cell calculated with B3LYP/def2-TZVPP.

Orbital #	Frontier Orbital #	Occupation	ε^{MO}-ε^{HOMO} / eV	Löwdin Reduced Orbital Population	Cu-d Löwdin Reduced Orbital Population / %
			alpha		
206	HOMO-78	1	-5.8	Cu(49%) His1(18%) His78(14%) Wat(10%)	48
213	HOMO-71	1	-5.5	Cell(35%) Cu(25%) His78(19%)	25
214	HOMO-70	1	-5.4	Cell(32%) His1(25%) Cu(20%) Wat(12%)	20
218	HOMO-66	1	-5.2	Cu(58%) Cell(16%) His1(10%)	58
223	HOMO-61	1	-4.9	Cu(42%) Cell(21%) Tyr(15%)	41
284	HOMO	1	0.0	Tyr(95%)	0
285	LUMO	0	4.4	Wat(33%) Cell(24%) His78(12%)	2

Table S9 (continued): Copper orbitals with significant d-orbital contribution, HOMO and LUMO in Cu(II)-Cell calculated with B3LYP/def2-TZVPP.

			Beta		
214	HOMO-69	1	-5.3	Cu(40%) His1(24%) His78(21%)	40
219	HOMO-64	1	-5.1	His78(36%) Cu(24%) His1(17%)	23
221	HOMO-62	1	-4.9	His1(40%) Cu(32%)	32
225	HOMO-58	1	-4.6	Cu(43%) Tyr(29%) His1(11%)	43
235	HOMO-48	1	-4.2	Cu(49%) Cell(14%) His78(12%)	47
240	HOMO-43	1	-4.0	His1(32%) Cu(25%) His78(14%) Tyr(11%)	21
283	HOMO	1	0.0	Tyr(93%)	1
284	LUMO	0	1.0	Cu(62%) His1(22%)	60

Table S10: Copper orbitals with significant d-orbital contribution, HOMO and LUMO in Cu(I)-Cell calculated with B3LYP/def2-TZVPP.

Orbital #	Frontier Orbital #	Occupation	ε^{MO}-ε^{HOMO} / eV	Löwdin Reduced Orbital Population	Cu-d Löwdin Reduced Orbital Population / %
266	HOMO-18	2	-2.2	His1(50%) Cu(29%)	26
274	HOMO-10	2	-1.4	Cu(51%) His1(40%)	51
275	HOMO-9	2	-1.3	Cu(65%) His78(18%)	65
277	HOMO-7	2	-1.2	Tyr(53%) Cu(27%)	26
278	HOMO-6	2	-1.2	Tyr(35%) Cu(24%) His78(18%) His147(11%)	23
279	HOMO-5	2	-1.1	Cu(49%) His1(34%)	49
280	HOMO-4	2	-1.0	Cu(53%) His78(22%) His1(14%)	52
281	HOMO-3	2	-0.7	Cu(72%) His78(17%)	70
282	HOMO-2	2	-0.3	Cu(55%) His1(25%) His147(12%)	50
284	HOMO	2	0.0	Tyr(90%)	5
285	LUMO	0	4.8	Wat(31%) Cell(24%) His1(23%)	3

Table S11: Copper orbitals with significant d-orbital contribution, HOMO and LUMO in Cu(I)…H_2O_2 calculated with B3LYP/def2-TZVPP.

Orbital #	Frontier Orbital #	Occupation	ε^{MO}-ε^{HOMO} / eV	Löwdin Reduced Orbital Population	Cu-d Löwdin Reduced Orbital Population / %
149	HOMO-10	2	-1.7	Cu(78%) His1(14%)	78
150	HOMO-9	2	-1.7	Cu(48%) His147(23%) His1(14%) His78(10%)	48
151	HOMO-8	2	-1.6	Cu(65%) His1(29%)	65
152	HOMO-7	2	-1.4	Cu(44%) His1(35%) His78(10%)	42
153	HOMO-6	2	-1.4	Cu(72%) His1(17%)	70
156	HOMO-3	2	-1.2	His78(60%) Cu(26%)	26
159	HOMO	2	0.0	Cu(59%) His1(26%)	52
160	LUMO	0	3.9	H2O2(82%)	6

Table S12: Copper orbitals with significant d-orbital contribution, HOMO and LUMO in Cu(I)-Cell…H_2O_2 calculated with B3LYP/def2-TZVPP.

Orbital #	Frontier Orbital #	Occupation	ε^{MO}-ε^{HOMO} / eV	Löwdin Reduced Orbital Population	Cu-d Löwdin Reduced Orbital Population / %
268	HOMO-20	2	-2.3	His1(42%) Cu(37%)	34
272	HOMO-16	2	-1.9	Cu(91%)	91
275	HOMO-13	2	-1.7	Cu(71%) His78(12%) His1(10%)	71
278	HOMO-10	2	-1.6	Cu(40%) His147(25%) His78(13%)	38
279	HOMO-9	2	-1.5	His147(45%) Cu(35%)	33
281	HOMO-7	2	-1.3	Cu(66%) His78(14%)	63
286	HOMO-2	2	-0.5	Cu(48%) His1(34%) H2O2(11%)	44
288	HOMO	2	0.0	Tyr(94%)	2
289	LUMO	0	2.6	H2O2(79%) Cu(12%)	11

Table S13: Copper orbitals with significant d-orbital contribution, frontier O_2 orbitals, HOMO and LUMO in Cu(I)…O_2 calculated with B3LYP/def2-TZVPP.

Orbital #	Frontier Orbital #	Occupation	ε^{MO}-ε^{HOMO} / eV	Löwdin Reduced Orbital Population	Cu-d Löwdin Reduced Orbital Population / %
			alpha		
144	HOMO-15	1	-2.9	His1(30%) Tyr(26%) Cu(24%) Wat(13%)	23
148	HOMO-11	1	-1.9	Cu(94%)	94
149	HOMO-10	1	-1.9	Cu(75%) His78(15%)	75
151	HOMO-8	1	-1.8	Cu(55%) His1(24%) His147(13%)	54
152	HOMO-7	1	-1.6	Cu(77%) His1(14%)	74
158	HOMO-1	1	-0.4	Cu(55%) His1(34%)	47
159	HOMO	1	-0.2	Tyr(91%)	4
160	LUMO	0	4.8	Wat(42%) Cu(20%) His78(16%) His1(14%)	7
			beta		
142	HOMO-15	1	-2.8	His1(34%) Wat(29%) Cu(21%)	20
146	HOMO-11	1	-1.9	Cu(78%)	78
147	HOMO-10	1	-1.8	Cu(76%)	76
148	HOMO-9	1	-1.8	His147(74%) Cu(20%)	20
149	HOMO-8	1	-1.7	Cu(55%) His1(31%)	54
150	HOMO-7	1	-1.6	Cu(75%) His1(17%)	73
157	HOMO	1	0.0	Cu(56%) His1(24%)	47
158	LUMO	0	1.0	O2(87%)	7
159	LUMO+1	0	1.2	O2(97%)	0

Table S14: Copper orbitals with significant d-orbital contribution, frontier O_2 orbitals, HOMO and LUMO in Cu(I)-Cell…O_2 calculated with B3LYP/def2-TZVPP.

Orbital #	Frontier Orbital #	Occupation	ε^{MO}-ε^{HOMO} / eV	Löwdin Reduced Orbital Population	Cu-d Löwdin Reduced Orbital Population / %
			alpha		
256	HOMO-32	1	-3.0	Cell(42%) Cu(23%) O2(12%) His1(11%)	22
260	HOMO-28	1	-2.8	O2(46%) Cell(31%)	2
269	HOMO-19	1	-2.2	Cu(86%)	86
272	HOMO-16	1	-2.0	Cu(55%) His78(13%) Gln162(12%)	55
274	HOMO-14	1	-1.9	Cu(70%) His1(16%)	66
278	HOMO-10	1	-1.6	Cu(28%) His147(25%) Cell(19%) His78(16%)	27
279	HOMO-9	1	-1.6	Cell(59%) Cu(24%)	22
286	HOMO-2	1	-0.9	His1(64%) Cu(23%)	21
288	HOMO	1	0.0	Tyr(95%)	1
289	LUMO	0	5.2	His1(83%)	1

Table S14 (continued): Copper orbitals with significant d-orbital contribution, frontier O_2 orbitals, HOMO and LUMO in Cu(I)-Cell…O_2 calculated with B3LYP/def2-TZVPP.

Orbital #	Frontier Orbital #	Occupation	ε^{MO}-ε^{HOMO} / eV	Löwdin Reduced Orbital Population	Cu-d Löwdin Reduced Orbital Population / %
			beta		
264	HOMO-22	1	-2.3	His1(34%) Cu(32%) Cell(22%)	31
269	HOMO-17	1	-2.1	Cu(59%) Cell(19%) Gln162(14%)	59
270	HOMO-16	1	-2.0	Gln162(73%) Cu(20%)	20
271	HOMO-15	1	-1.9	Cu(68%) His78(15%) His1(10%)	67
274	HOMO-12	1	-1.7	Cu(61%) His1(17%)	58
278	HOMO-8	1	-1.5	Cu(63%) His78(11%) His1(11%)	60
284	HOMO-2	1	-0.3	Cu(45%) O2(25%) His1(20%)	40
286	HOMO	1	0.0	Tyr(92%)	2
287	LUMO	0	1.8	O2(67%) Cu(22%)	22
288	LUMO+1	0	2.1	O2(90%)	0

Table S15: Copper orbitals with significant d-orbital contribution, frontier O_2 orbitals, HOMO and LUMO in Cu(II)-O_2 calculated with B3LYP/def2-TZVPP.

Orbital #	Frontier Orbital #	Occupation	ε^{MO}-ε^{HOMO} / eV	Löwdin Reduced Orbital Population	Cu-d Löwdin Reduced Orbital Population / %
			alpha		
136	HOMO-23	1	-3.7	Cu(40%) His78(19%) His1(16%) Tyr(11%)	39
137	HOMO-22	1	-3.7	Cu(39%) His1(28%) Gln162(10%)	38
140	HOMO-19	1	-3.4	Cu(31%) His78(27%) His1(25%) Tyr(12%)	29
142	HOMO-17	1	-3.1	Cu(87%)	87
144	HOMO-15	1	-2.8	Cu(49%) His78(34%)	48
146	HOMO-13	1	-2.5	Cu(47%) Tyr(15%) His1(11%)	44
148	HOMO-11	1	-2.3	His1(42%) Cu(36%)	35
149	HOMO-10	1	-2.1	O2(64%) Gln162(29%)	2
150	HOMO-9	1	-1.9	Gln162(49%) O2(37%)	2
151	HOMO-8	1	-1.8	O2(42%) His1(25%) Gln162(16%)	7
157	HOMO-2	1	-0.8	O2(32%) Cu(30%) His1(28%)	29
159	HOMO	1	-0.1	His147(97%)	0
160	LUMO	0	5.1	His1(64%) Wat(19%)	3

Table S15 (continued): Copper orbitals with significant d-orbital contribution, frontier O_2 orbitals, HOMO and LUMO in Cu(II)-O_2 calculated with B3LYP/def2-TZVPP.

			beta		
138	HOMO-19	1	-3.5	Tyr(35%) His78(27%) Cu(25%)	25
141	HOMO-16	1	-3.0	His1(43%) Cu(33%) Tyr(11%)	31
143	HOMO-14	1	-2.7	Cu(81%)	80
144	HOMO-13	1	-2.6	Cu(70%) His78(20%)	70
147	HOMO-10	1	-2.2	Cu(51%) His1(30%)	49
148	HOMO-9	1	-2.1	Cu(52%) His1(34%)	49
157	HOMO	1	0.0	O2(40%) Cu(27%) Tyr(16%) His1(10%)	23
158	LUMO	0	2.5	O2(49%) Cu(35%)	34
159	LUMO+1	0	2.8	O2(91%)	2

Table S16: Copper orbitals with significant d-orbital contribution, frontier O_2 orbitals, HOMO and LUMO in Cu(II)-Cell-O_2 calculated with B3LYP/def2-TZVPP.

Orbital #	Frontier Orbital #	Occupation	ε^{MO}-ε^{HOMO} / eV	Löwdin Reduced Orbital Population	Cu-d Löwdin Reduced Orbital Population / %
			alpha		
242	HOMO-46	1	-3.8	Cu(38%) His1(21%) Tyr(15%)	36
244	HOMO-44	1	-3.8	Tyr(34%) Cu(26%) Gln162(15%)	26
247	HOMO-41	1	-3.6	Cu(34%) Tyr(32%) His78(12%) Gln162(10%)	34
251	HOMO-37	1	-3.3	Cell(51%) Cu(20%) Wat(12%)	20
252	HOMO-36	1	-3.3	Cu(39%) Tyr(23%) His1(14%)	38
256	HOMO-32	1	-3.1	Wat(35%) Cu(32%) His1(12%)	31
260	HOMO-28	1	-2.8	His78(39%) Cu(25%) Cell(20%)	24
265	HOMO-23	1	-2.6	Cu(34%) His1(23%) His78(17%) Cell(12%)	33
267	HOMO-21	1	-2.4	Cu(37%) Tyr(20%) Gln162(15%) His1(14%)	34
273	HOMO-15	1	-1.9	O2(85%)	2
274	HOMO-14	1	-1.7	O2(32%) His1(31%) Cell(15%)	7
285	HOMO-3	1	-0.8	O2(31%) His1(30%) Cu(15%) Tyr(11%)	15
288	HOMO	1	0.0	Tyr(94%)	1
289	LUMO	0	5.3	His1(83%)	1

Table S16 (continued): Copper orbitals with significant d-orbital contribution, frontier O_2 orbitals, HOMO and LUMO in Cu(II)-Cell-O_2 calculated with B3LYP/def2-TZVPP.

Orbital #	Frontier Orbital #	Occupation	ε^{MO}-ε^{HOMO} / eV	Löwdin Reduced Orbital Population	Cu-d Löwdin Reduced Orbital Population / %
			beta		
238	HOMO-48	1	-3.9	Cu(28%) His78(23%) His1(19%) Cell(11%)	25
248	HOMO-38	1	-3.5	Tyr(35%) Cu(29%) His78(16%)	29
257	HOMO-29	1	-2.9	Cu(45%) Cell(21%) His1(14%) Wat(10%)	44
260	HOMO-26	1	-2.7	Cu(58%) His1(17%) His78(15%)	56
263	HOMO-23	1	-2.6	Cu(36%) His78(19%) Tyr(18%)	35
266	HOMO-20	1	-2.3	Cu(52%) His1(24%)	51
271	HOMO-15	1	-2.0	Cu(38%) His1(27%) Cell(13%)	34
284	HOMO-2	1	-0.1	O2(47%) Cu(22%) Tyr(13%) His1(10%)	18
286	HOMO	1	0.0	Tyr(79%)	5
287	LUMO	0	2.4	Cu(45%) O2(36%)	44
288	LUMO+1	0	2.8	O2(91%)	1

Table S17: Copper orbitals with significant d-orbital contribution, frontier Cl^- orbitals, HOMO and LUMO in Cu(II)-Cell-Cl^- calculated with B3LYP/def2-TZVPP.

Orbital #	Frontier Orbital #	Occupation	ε^{MO}-ε^{HOMO} / eV	Löwdin Reduced Orbital Population	Cu-d Löwdin Reduced Orbital Population / %
			alpha		
193	HOMO-95	1	-6.5	His1(34%) Cu(32%) His78(24%)	32
219	HOMO-69	1	-5.2	His1(41%) Cu(25%) Cl(13%)	22
223	HOMO-65	1	-4.9	His1(51%) Cu(25%) His78(13%)	25
225	HOMO-63	1	-4.9	His78(23%) His1(21%) Cu(20%) Cell(17%)	20
232	HOMO-56	1	-4.5	Cu(31%) His147(27%) His1(15%)	31
233	HOMO-55	1	-4.4	Cu(58%) Tyr(15%)	57
236	HOMO-52	1	-4.2	Cu(30%) His1(28%) Cell(15%) Wat(14%)	29
246	HOMO-42	1	-3.7	Cu(29%) His78(18%) Wat(17%) His1(10%)	26
267	HOMO-21	1	-2.4	Gln162(58%) Cl(20%)	3
273	HOMO-15	1	-1.9	Cl(54%) His78(16%)	3
274	HOMO-14	1	-1.7	Cl(39%) Gln162(36%)	2
288	HOMO	1	0.0	His147(96%)	0
289	LUMO	0	5.3	His1(79%)	1

Table S17 (continued): Copper orbitals with significant d-orbital contribution, frontier Cl^- orbitals, HOMO and LUMO in Cu(II)-Cell-Cl^- calculated with B3LYP/def2-TZVPP.

Orbital #	Frontier Orbital #	Occupation	ε^{MO}-ε^{HOMO} / eV	Löwdin Reduced Orbital Population	Cu-d Löwdin Reduced Orbital Population / %
			beta		
225	HOMO-62	1	-4.6	Cell(34%) Cu(24%) His1(13%)	24
236	HOMO-51	1	-4.1	Cu(50%) Cell(20%) His78(11%)	50
239	HOMO-48	1	-3.9	Wat(39%) Cu(37%)	37
240	HOMO-47	1	-3.9	Cell(44%) Wat(25%) Cu(21%)	21
260	HOMO-27	1	-2.8	Cell(40%) Cu(22%)	21
265	HOMO-22	1	-2.5	His1(34%) Cu(23%)	22
267	HOMO-20	1	-2.3	Gln162(26%) Cl(22%) Wat(22%) His1(12%)	4
273	HOMO-14	1	-1.8	Cl(49%) His78(16%) Gln162(14%)	4
274	HOMO-13	1	-1.7	Cl(38%) Gln162(18%) Cell(14%)	2
287	HOMO	1	0.0	His147(96%)	0
288	LUMO	0	2.4	Cu(59%) His1(14%) Cl(14%)	58

Table S18: Copper orbitals with significant d-orbital contribution, frontier Cl^- orbitals, HOMO and LUMO in Cu(I)-Cell-Cl^- calculated with B3LYP/def2-TZVPP.

Orbital #	Frontier Orbital #	Occupation	ε^{MO}-ε^{HOMO} / eV	Löwdin Reduced Orbital Population	Cu-d Löwdin Reduced Orbital Population / %
281	HOMO-7	2	-0.9	Cu(55%) Tyr(29%)	53
282	HOMO-6	2	-0.9	Cu(86%)	86
283	HOMO-5	2	-0.9	Cl(68%) Cu(10%)	10
284	HOMO-4	2	-0.8	Cu(65%) His1(10%)	65
285	HOMO-3	2	-0.5	Tyr(46%) Cu(41%)	41
286	HOMO-2	2	-0.4	Cu(72%) Tyr(12%)	70
288	HOMO	2	0.0	Cu(72%) His1(18%)	66
289	LUMO	0	4.7	Cell(47%) Wat(39%)	0

References

1. V. V. Vu and S. T. Ngo, *Coordination Chemistry Reviews*, 2018, **368**, 134-157.
2. H. Lim, M. T. Brueggemeyer, W. J. Transue, K. K. Meier, S. M. Jones, T. Kroll, D. Sokaras, B. Kelemen, B. Hedman, K. O. Hodgson and E. I. Solomon, *J Am Chem Soc*, 2023, **145**, 16015-16025.
3. C. H. Kjaergaard, M. F. Qayyum, S. D. Wong, F. Xu, G. R. Hemsworth, D. J. Walton, N. A. Young, G. J. Davies, P. H. Walton, K. S. Johansen, K. O. Hodgson, B. Hedman and E. I. Solomon, *Proc Natl Acad Sci U S A*, 2014, **111**, 8797-8802.
4. G. Courtade, L. Ciano, A. Paradisi, P. J. Lindley, Z. Forsberg, M. Sorlie, R. Wimmer, G. J. Davies, V. G. H. Eijsink, P. H. Walton and F. L. Aachmann, *Proc Natl Acad Sci U S A*, 2020, **117**, 19178-19189.
5. M. M. Hagemann and E. D. Hedegard, *Chemistry*, 2023, **29**, e202202379.
6. E. D. Hedegard and U. Ryde, *ACS Omega*, 2017, **2**, 536-545.
7. S. Kim, J. Stahlberg, M. Sandgren, R. S. Paton and G. T. Beckham, *Proc Natl Acad Sci U S A*, 2014, **111**, 149-154.
8. L. Bertini, R. Breglia, M. Lambrughi, P. Fantucci, L. De Gioia, M. Borsari, M. Sola, C. A. Bortolotti and M. Bruschi, *Inorg Chem*, 2018, **57**, 86-97.
9. E. D. Hedegard and U. Ryde, *Chem Sci*, 2018, **9**, 3866-3880.
10. K. E. Frandsen, T. J. Simmons, P. Dupree, J. C. Poulsen, G. R. Hemsworth, L. Ciano, E. M. Johnston, M. Tovborg, K. S. Johansen, P. von Freiesleben, L. Marmuse, S. Fort, S. Cottaz, H. Driguez, B. Henrissat, N. Lenfant, F. Tuna, A. Baldansuren, G. J. Davies, L. Lo Leggio and P. H. Walton, *Nat Chem Biol*, 2016, **12**, 298-303.